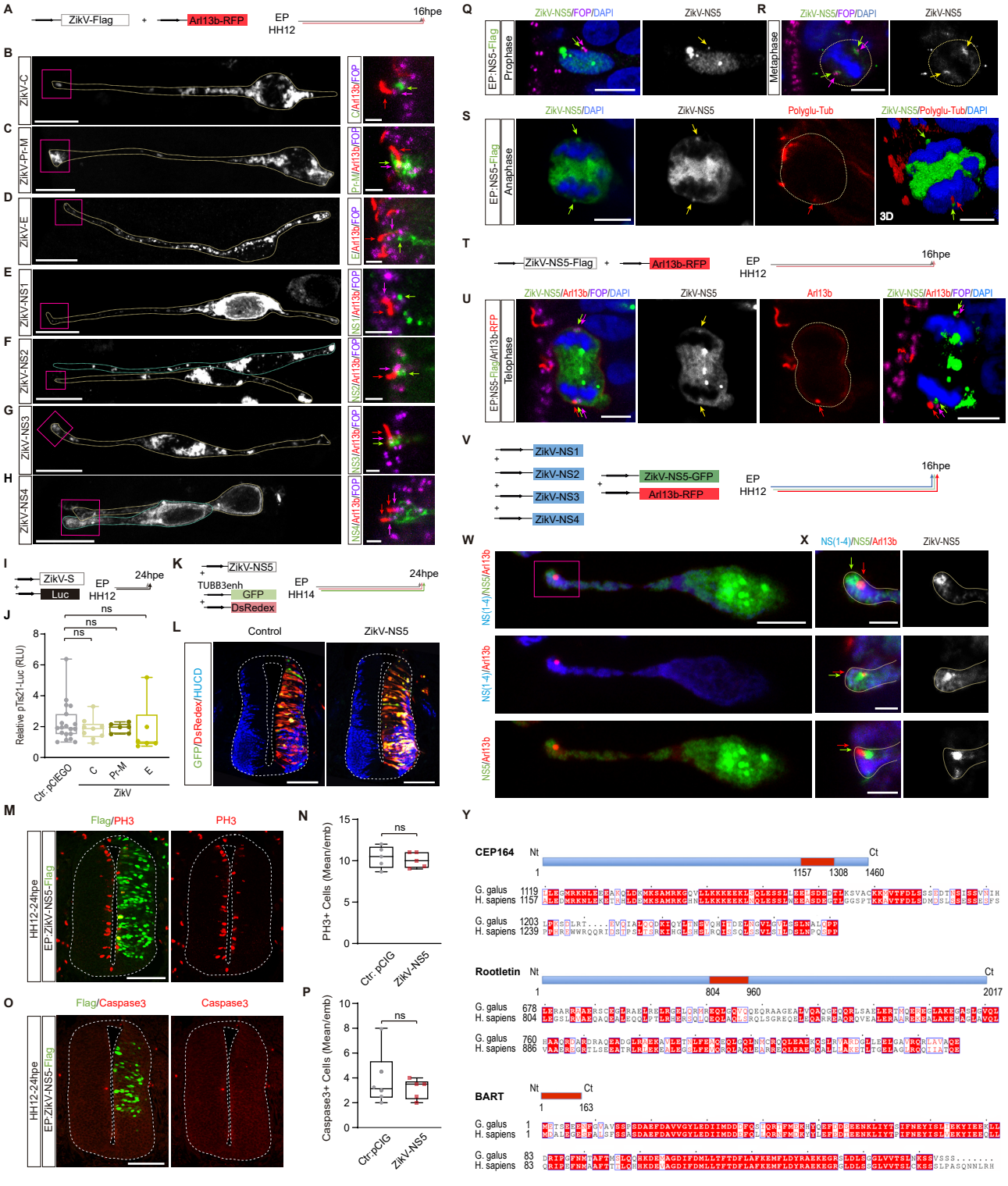

-Saade et al-Figure S1-

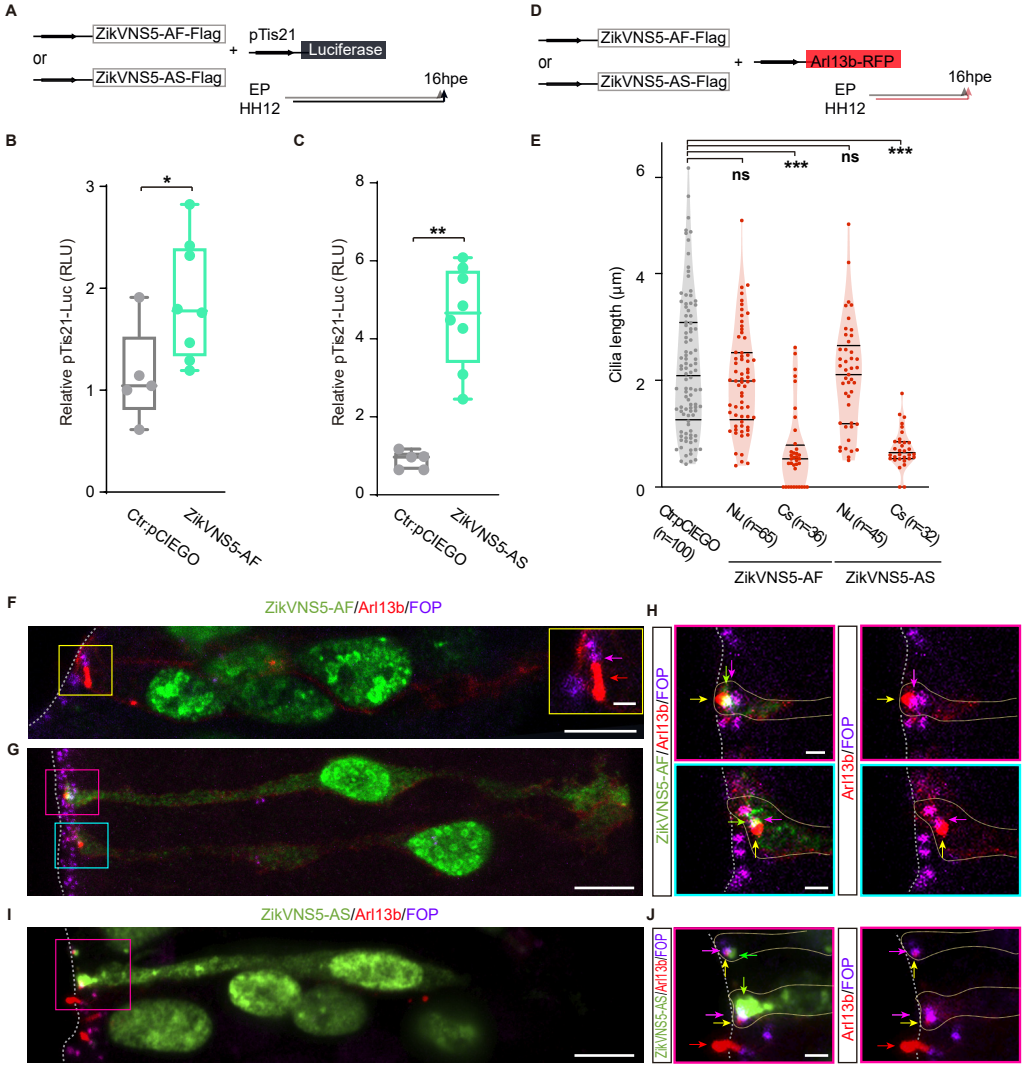

-Saade et al- Figure S2-

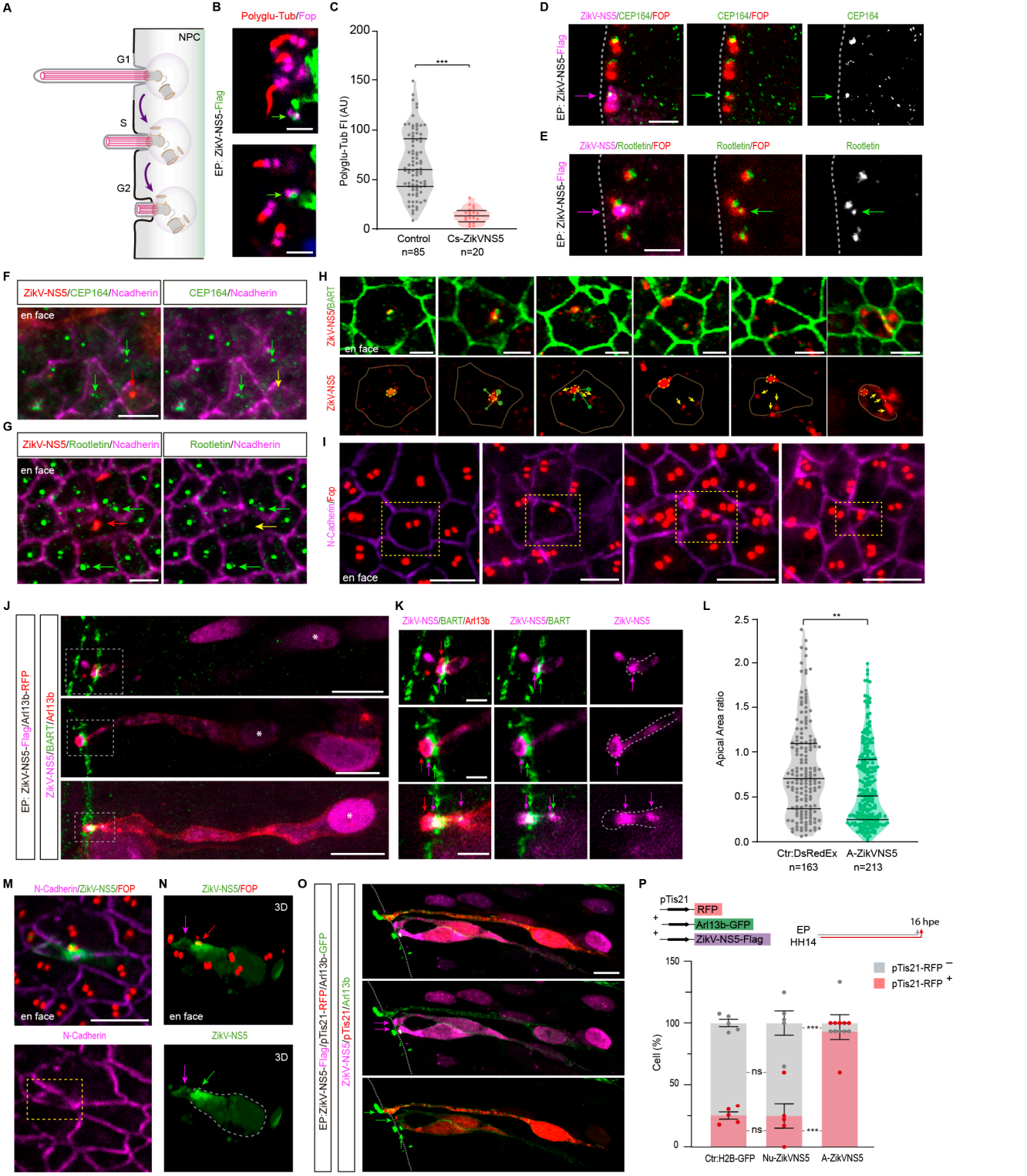

-Saade et al-Figure S3-

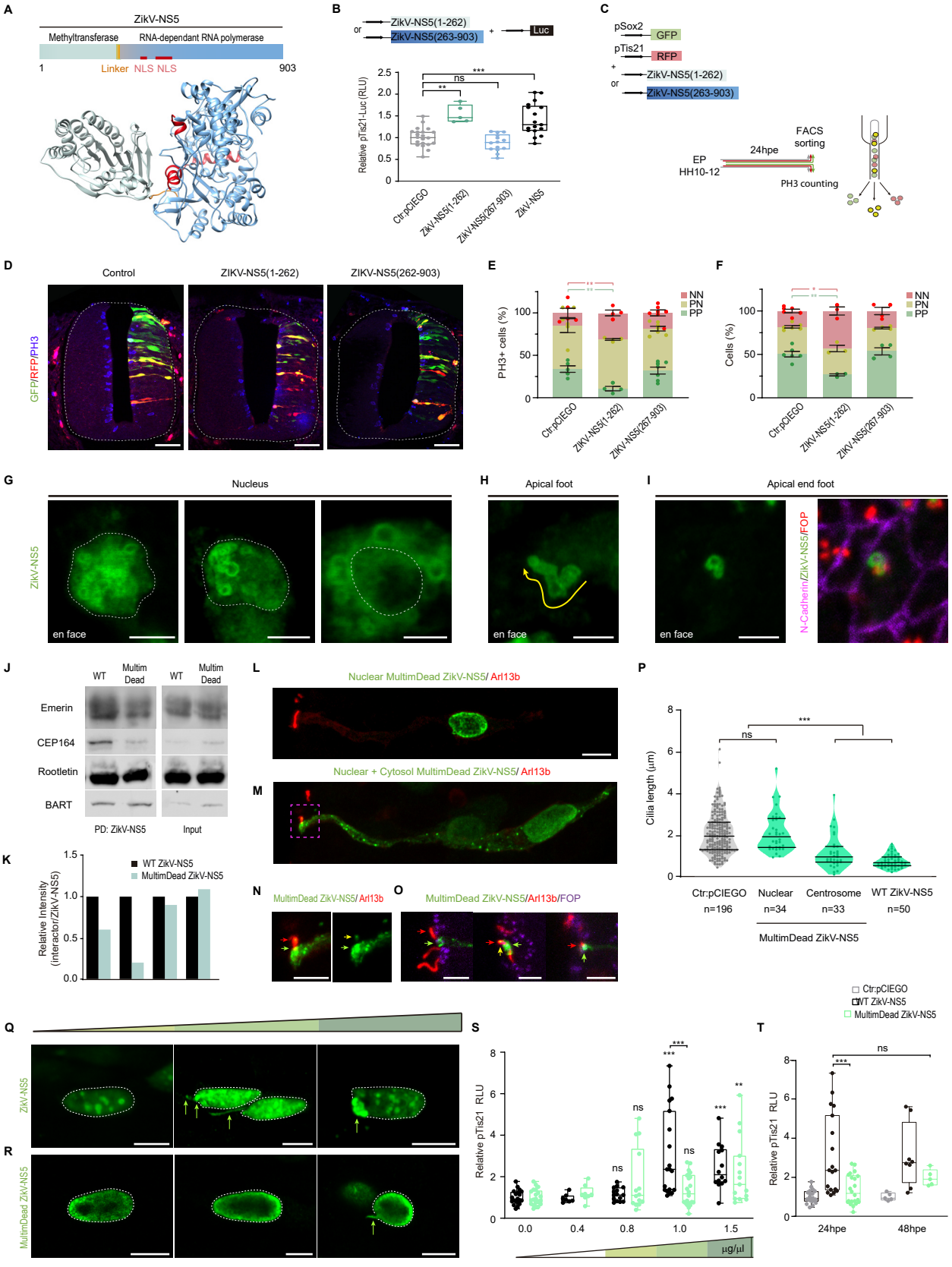

-Saade et al-Figure S4-

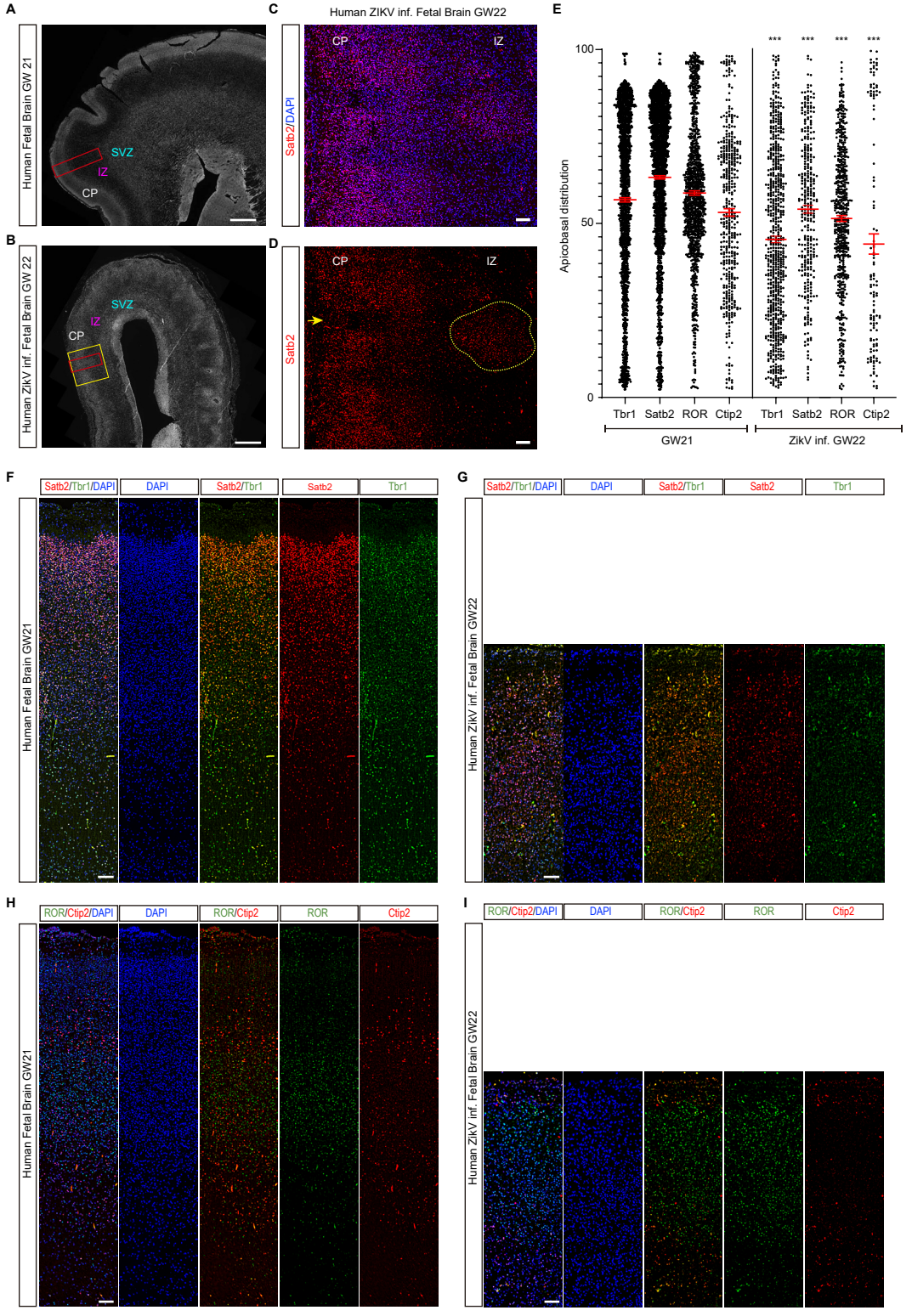

-Saade et al-Figure S5-

Supplemental figures legends

Figure S1. (Related to Figure 1 and Figure 2); *ZikV-NS5 interacts with centrosomal proteins*

(A) Scheme showing the DNAs co-electroporated for immunohistochemistry.

(B-H) Subcellular localization of ZikV structural (C, Pr-M, E) and non-structural (NS) proteins co-electroporated with the cilia marker Arl13b-RFP (red) into stage HH12 chick embryos. At 16 hours post-electroporation (hpe) viral proteins were detected using an anti-FLAG antibody and visualized by confocal microscopy. In electroporated NPCs, ZikV-NS1 (**E**) and ZikV-NS2 (**F**) are located in the cytoplasm, excluded from the nucleus, the FOP labelled (purple) centrosome and the Arl13b-RFP (red) labelled cilia. ZikV-Pre-M (**C**) and ZikV-NS3 (**G**) have a cytoplasmic distribution and they accumulate at the cilia base without affecting cilia integrity. ZikV-NS4 (**H**) localizes at the membrane and it is excluded from the FOP labelled centrosome.

(**I, J**) Quantification of the Luc/Renilla activity of the pTis21-Luc reporter after electroporation of the empty vector pCIEGO or the ZikV structural proteins (ZikV-S) DNAs indicated (plots show the mean ± SD, n=6-13 embryos/condition)

(**K, L**) Scheme showing the DNAs co-electroporated for immunohistochemistry (**K**). Representative images of spinal cord sections from chick embryo (stage HH12+24hpe), showing the electroporation of control (red) of ZikV-NS5 (red), Tubb3enh (green) and HUC/D (blue) immunostaining of differentiated neurons (**L**).

(M) Representative images of spinal cord sections from a chick embryo (stage HH12+24hpe), showing ZikV-NS5-FLAG (green) electroporation and anti-PH3 immunostaining (red). **(N)** Quantification of $pH3^+$ cells in the electroporated control vs ZIKV-NS5 electroporated NT (Ctr median=10.5 ± 1.3 vs ZIKV-NS5 median= 10 ± 0.9 $pH3^+$ cells, n=5 embryos)

(O) Representative images of spinal cord sections from a chick embryo (stage HH12+24hpe), showing ZikV-NS5-FLAG (green) electroporation and anti-Caspase 3 immunostaining (red). **(P)** Quantification of Caspase 3^+ cells in the electroporated control and ZIKV-NS5 electroporated NT (Ctr median=3 ± 2.2 vs ZIKV-NS5 median=3.5 ± 1 Caspase 3^+ cells, n=5-6 embryos)

(Q-U) ZikV-NS5 localizes to the centrosomes at different mitotic phases. (**Q**) ZikV-NS5-FLAG revealed by anti-FLAG staining (green) at centrosomes labelled with anti-FOP (purple) at prophase. DAPI (blue) labels the chromosomes and the arrows point to the centrosomes. **(R)** ZikV-NS5-FLAG (green) localizes symmetrically to the centrosomes during metaphase. **(S-U)** ZikV-NS5-FLAG (green) localizes to centrosomes during anaphase and telophase. The mother centrosome is labelled with anti-polyglutamylated Tubulin (red) (**S**) and Arl13b (red) (**T, U**). **(V-X)** Scheme showing the DNAs co-electroporated for immunohistochemistry (**V**). Subcellular localization of ZikV-NS1-4 proteins co-electroporated with ZikV-NS5-GFP (green) and with the cilia marker Arl13b-RFP (red) in stage HH12 chick embryos (**W**). At 16 hpe viral proteins were detected using anti-FLAG antibody and visualised by confocal microscopy. In electroporated NPCs, ZikV-NS5 (green) remained associated to the cilia base identified by Arl13b-RFP (red) (**X**).

(Y) Sequence alignment highlighting the conservation between human and chicken proteins in the ZikaV-NS5-interaction domain (red box)

ns: not significant. one-way ANOVA- Kruskal-Wallis test **J,** Mann-Whitney *U* test, **N, P**. Scale bars 9 μm (**B**-**H**), 2 μm (inset **B**-**H**, **X**), 75 μm (**L**), 70 μm (**M**, **O**), 5 μm (**Q**-**S, U**), 6 μm (**W**)

Figure S2 (Related to Figure 1 and Figure 2); *ZikV-NS5 protein form different viral strains behave similarly in NPCs*

(A) Scheme showing the ZikV-NS5 DNAs from the African (AF) and the Asian (AS) strains electroporated for Luciferase assay.

(B, C) Quantification of the Luc/Renilla activity of the pTis21-Luc reporter after electroporation of the control empty vector pCIEGO or the African strain ZikV-NS5-AF (plots show the mean ± SD, n=5-8 embryos/condition) (**B**). Quantification of the Luc/Renilla activity of the pTis21-Luc reporter after electroporation of the control empty vector pCIEGO or the Asian strain ZikV-NS5-AS (plots show the mean ± SD, n=5-8 embryos/condition) (**C**).

(D) Scheme showing the strains specific ZikV-NS5 co-electroporated with the pan-cilia marker Arl13b for immunohistochemistry and cilia length measurement.

(E) Violin plots of cilia length in NPCs electroporated with the pCIEGO empty vector (control), in NPCs electroporated with ZikV-NS5-AF or ZikV-NS5-AS. Measurements have been performed according to the subcellular localization of ZikV-NS5 exclusively

in the nucleus (Nu-ZikV-NS5) or localized to the centrosome at the cilia base (Cs-ZikV-NS5).

(F-H) Selected images show the Arl13b-RFP labelled cilia (red arrows) and FOP stained centrosomes (purple arrows) lining the NT lumen (dotted line), and the localization of the ZikV-NS5-AF: exclusively in the nucleus **(F)** with normal cilia integrity **(**inset **F,** red arrow**),** and localized to the cilia base (green arrows) and associated to ciliopathy **(G,** yellow arrows **H).**

(I-J) Selected images show the Arl13b-RFP labelled cilia (red arrows) and FOP stained centrosomes (purple) lining the NT lumen (dotted line), and the localization of the ZikV-NS5-AS: exclusively in the nucleus **(I)** with normal cilia integrity **(J**, red arrow**),** and localized to the cilia base (**I**, green arrows **J**) and associated to ciliopathy **(I,** yellow arrows **J).**

In violin plots, the upper and lower lines indicate the interquartile range, and the middle line the median. ***p<0.001, **p<0.01, *P<0.05, ns: not significant. Mann-Whitney U test **B, C.** one-way ANOVA- Kruskal-Wallis test **E**. Scale bars 7 μm (**F, G, I**), 1 μm (inset **F, H, J**).

Figure S3 (Related to Figure 2 and Figure 4); *ZikV-NS5 localization to the cilium base impairs cilia elongation and promotes neural delamination*

(A) The scheme depicts the cilia length in relation to cell cycle phases of dividing NPCs, with the microtubules in cilia highlighted in red.

(B) Selected images show Polyglutamylated-tubulin labelled cilia (red) and FOP stained centrosomes lining the NT lumen (dotted line), in control and ZikV-NS5-FLAG electroporated embryos (green, arrow pointed)

(C) Violin plots of the cilia length in NPCs electroporated with ZikV-NS5, in which the protein is localized to the centrosome at the the cilia base (Cs-ZikV-NS5). Non-electroporated neighbour NPCs (spaced by one cell distance from the ZikV-NS5 electroporated NPCs) are used as control of cilia length in Wild-type.

(the upper and lower lines indicate the interquartile range, the middle line the median)

(D, E) Selected images show ZikV-NS5-FLAG (purple arrow) co-localized to FOP stained centrosomes (red) and to the CEP164 stained mother centriole (green arrow, **D**) or Rootletin staining (green arrow, **E)**

(F) *En face* images of N-cadherin labelled AJs (purple), endogenous CEP164 (green) labelled centrosomes and ZikV-NS5-FLAG subcellular localization (red arrow)

(G) *En face* images of N-cadherin labelled AJs (purple), endogenous Rootletin (green) labelled centrosomes, and ZikV-NS5-FLAG subcellular localization (red arrow). The yellow arrow points to a centrosome where CEP164 and Rootletin expression is reduced relative to the neighbouring NPCs.

(H) *En face* images of endogenous apical BART (green) and ZikV-NS5-FLAG subcellular localization (red). Green lines and yellow arrows point to BART and ZikV-NS5 de-localization from the centrosome towards the apical belt, respectively. Centrosomal ZIKV-NS5 is highlighted with a yellow dashed circle.

(I) *En face* images of N-cadherin (purple) and FOP stained centrosomes (red) in wild-type embryos. Lateral positioned centrosomes are correlated to the apical area restriction.

(J) Representative images of ZikV-NS5-FLAG (purple) co-localization with Arl13b (red) and with endogenous BART (green) lining the NT lumen. **(K)** Boxed areas in j, green arrows point to BART localization at the apical belt, red arrows to Arl13bshort cilia, purple arrows to ZikV-NS5 at the centrosome and apical abscising area.

(L) Violin plots of the ratio of the apical area (AA) in NPCs expressing DsRedEx (control) in comparison to NPCs presenting an apical distribution of ZikV-NS5 (A-ZikV-NS5)(the upper and lower lines indicate the interquartile range, and the middle line the median).**(M,N)** *En face* and 3D images of a NPC where N-cadherin labelled AJs (purple), FOP labelled centrosome (red) and the ZikV-NS5-FLAG subcellular localization (green). The purple arrow points to the apical area, the red arrow to a laterally positioned centrosome, the green arrow to ZikV-NS5 at the centrosome.

(O) Representative images of ZikV-NS5-FLAG (purple) electroporated NPCs in which ZikV-NS5-FLAG was located at the cilium base, as determined by Arl13b-GFP (green arrows) and correlated with pTis21-RFP (red) expression.

(P) Scheme of electroporated DNAs and quantification of the proportion of pTis21-RFP^+ cells in wild-type (H2B-GFP+ NPCs) and according to the nuclear (Nu) or apical (A) distribution of ZikV-NS5 (the error bars correspond to the mean ± s.e.m.)

***p<0.001, **p<0.01; exact P values 0.0011 (**L**), *P<0.05, ns: not significant. **C**, **L** Mann-Whitney U test; **P**, one-way ANOVA. Scale bars 2 μm (**B**, **D**, **E**, **K**), 4 μm (**F**-**I, M**). 7 μm (**J, O**).

Figure S4 (Related to Figure 4); *The multimeric arrangement of ZikV-NS5 is required for its localization to the cilia base and the promotion of neurogenic divisions*

(A) The scheme depicts the MTase (light blue) and RdRp (dark blue) domains in the ZikV-NS5 protein, with the linker highlighted in yellow. 3D representation of one ZikV-NS5 monomer showing an orientation from the top of the RdRP, with the MTase domain in grey, and the RdRP fingers, palm and thumb domains in blue. Red indicates the position of the NLS.

(B) Quantification of the Luc/Renilla activity of the pTis21-Luc reporter after electroporation of the DNAs indicated (the plots show the mean ± s.e.m., n=6-8 embryos/condition)

(C) Scheme representing the reporter co-electroporation experiments, harvested at 24 hpe for either flow cytometry analysis or for anti-PH3 immunostaining.

(D) Selected images of pSox2+ (green) and pTirs21+ (red) NPCs, and pH3 stained mitoses (blue) in the control or ZikV-NS5 NT.

(E) Quantification of reporter-expressing $pH3^{+}$ dividing cells in each condition: PP ($pSox2^{+}/pTis21^{-}$, green), PN ($pSox2^{+}/pTis21^{+}$, yellow) and NN ($pSox2^{-}/pTis21^{+}$, red). The data represents the mean ± s.e.m)

(F) Quantification of reporter-expressing FACS sorted cells in each condition, the data representing the mean ± s.e.m.)

(G) Representatives *en face* images of ZikV-NS5-FLAG ring-like aggregates (green). The nucleus is highlighted with a dashed-dotted line

(H, I) Representative *en face* images of ZikV-NS5-FLAG (green) where the yellow arrow follows the basal to apical ring-like distribution of the protein all along the apical foot (**H**) and at the apical-end foot at the centrosome level (**i**). N-cadherin labelled AJs (purple) and the FOP labelled centrosome (red).

(**J, K**) HEK-293 cells were co-transfected with WT or MultimDead ZikV-NS5 and the DNAs indicated, and the cell extracts were analysed by western blots (**j**). Quantification of Pull-down (PD) assays (**K**) shows a less efficient binding of the MultimDead ZikV-NS5 to Cep164 and Emerin.

(L-O) Representative images of the MultimDead ZikV-NS5 subcellular localization associated with Arl13b labelled cilia (red) and FOP labelled centrosomes (blue). Ciliopathy (red arrow) associated with the MultimDead ZikV-NS5localization to the

cilium base (green arrow). MultimDead ZIKV-NS5 was also detected in the tip of cilia (yellow arrow).

(P) Violin plots of the cilia length in association with the subcellular localization of the MultimDead ZikV-NS5(the upper and lower lines indicate the interquartile range, the middle line the median).

(Q, R) Representative images of ZikV-NS5-FLAG nuclear aggregates (green arrow) associated with increasing electroporation. **(R)** MultimDead ZikV-NS5 only causes nuclear envelope disruption at high concentrations (green arrow).

(S, T) Quantification of the Luc/Renilla activity of the pTis21-Luc reporter after electroporation of the DNAs indicated (the plots show the mean ± SD, n=6-8 embryos/condition).

****p*<0.001, ***p*<0.01; exact *P* values 0.0015 (**E**) 0.0044 (**F**) 0.0051 (**S**), **P*<0.05; exact *P* values 0.049 (**E**), ns: not significant. **B**, **E**, **F, S, T** one-way ANOVA, **P**, Kruskal-Wallis test . Scale bars 30 μm (**D**), 3 μm (**G-I, N, O**). 5 μm (**L, M, Q, R**).

Figure S5. (Related to Figure 5); *Microcephaly in ZikV infected Human foetal brain is accompanied by reduced neuron numbers and cortical layer disorganization*

(A) Representative image of control GW21 forebrain coronal sections indicating the different forebrain areas. Red inset highlights the area quantified in **(e)** and the images shown in **(F)** and **(H)**.

(B) Representative image of ZikV infected GW22 forebrain coronal sections. Red box highlights the area quantified in **(E)** and the images shown in **(G)** and **(I)**.

(C, D) Representative image of the yellow inset in **b** immunostained with DAPI and the upper-layer neuronal marker Satb2. **(D)** Dashed line surrounds Satb2+ neuronal misplacement at the intermediate zone (IZ). Yellow arrow points to disrupted Satb2+ neuronal migration during cortical plate (CP) formation.

(E) Relative apicobasal position of Tbr1+, Satb2+, ROR+, or Ctip2+ neurons at GW21 and ZikV infected GW22. Values represent median ± s.e.m. Total number of neurons counted, GW21: Tbr1+ n = 1.595, Satb2+ n = 1.925, ROR+ n = 1.063, Ctip2+ n = 436; ZIKV inf. GW22: Tbr1+ n = 660, Satb2+ n = 329, ROR + n = 572, Ctip2+ n = 125.

(F, G) Representative image of the generating cortical plate and intermediate zone at GW21 (**D**) and ZikV infected GW2 (**e**), immunostained for marker of post-mitotic neurons Tbr1+ and upper-layer neurons, Satb2.

(H-I) Representative image of the generating cortical plate and intermediate zone at GW21 (**F**) and ZikV infected GW2 (**G**), immunostained for markers of deep-layer neurons, ROR and Ctip2.

All figures were digitally stitched by the appropriate image software as described in STAR Methods.

***p<0.001, **p<0.01, *P<0.05. **E**, Mann-Whitney *U* test. Scale bars 1.5 mm (**A**, **B**), 200 μm (**C,D**), 100 μm (**F-I**).